OPTIMIZED TRANSFER LEARNING PIPELINE USING RESNET-50 AND BAYESIAN OPTIMIZATION FOR OIL SPILLAGE DETECTION

Mitong Dorcas MITONGB@GMAIL.COM

Muhammad Bashir Abdullahi EL.BASHIR02@FUTMINNA.EDU.NG

Emmanuel Ogbonnia EMMANUEL.OGBONNIA@NILEUNIVERSITY.EDU.NG

Federal University of Technology Minna, Nigeria

Editor: Sakinat Folorunso, Roseline Ogundokun, and Francisca Oladipo

Abstract

The paper presents an efficient transfer-learning framework that combines a pretrained ResNet-50 backbone with Bayesian hyperparameter optimization and, therefore, it selects oil spills among the common oceanic look-alikes in Sentinel-1 SAR images. The architecture is a frozen convolutional feature extractor followed by a small classification head (Dense 256 Dropout Sigmoid), and the optimizer (SGD) is automatically tuned (0.001578), learning rate (0.001578), weight decay (0.012348), dropout (0.0129), and momentum (0.5872). With an imbalanced cohort consisting of a large proportion of non-oil manifestations of a dark spot, the refined model would achieve an accuracy of 85.36%, a weighted F1-score of 85.32, and balanced class-wise performance (Non-Oil F1= 0.89; Oil F1= 0.79). The training validation curves demonstrate consistent convergence without over-fitting and thus testify to the effectiveness of the Bayesian optimization technique in exploring the complex hyperparameter space of the SAR-based oil spill detection. In turn, the given framework is a driving force of operational monitoring since it provides a powerful discrimination between realistic spills and natural equivalents and maintains the computational efficiency that can be easily deployed in real-time.

Keywords: Oil Spill Detection, Synthetic Aperture Radar (SAR), Transfer Learning, ResNet-50, Bayesian Optimization, Hyperparameter Tuning.

1. INTRODUCTION

1.1. Background and Motivation

Marine oil spills are one of the most harmful environmental threats that are facing the modern marine ecosystems and bringing in the long-term harm to the marine biodiversity, coastal communities and world fisheries. Such incidents have ecological and economic implications that require the implementation of effective and swift detecting strategies to enable the response and mitigation. Spaceborne Synthetic Aperture Radar (SAR) has become one of the most significant technologies that are able to monitor the water in real time, all year round, and provide quality images that are not dependent upon a cloud cover or the sun as a source of light (Yang and Schütte, 2025). The Sentinel-1 system of the European Space Agency in particular, not only provides unmatched coverage of maritime areas in terms of time and space, but is also a treasure trove of operational oil spill monitoring.

1.2. The Challenge of Look-Alikes

1.2.1. Although the benefits of SAR are quite strong, proper detection of oil spills is a daunting task with the omnipresence of oceanic look-alikes, natural phenomena that mimic the radar backscatter pattern of an oil slick with perfect visual similarity. They are low-wind zones, biogenic surface films, internal waves, upwelling areas, and rain cells, all of which appear as dark areas in VV polarised SAR imagery in the same backscatter reduction processes (Yang and Schütte, 2025). The physical resemblance between such phenomena on the one hand and real oil spills on the other hand creates a complicated problem of classification, where the traditional threshold-based or manual interpretation techniques are often not sufficient.

1.3. Deep Learning and the Hyperparameter Optimization Challenge

The recent revolution in deep learning and specifically in Convolutional Neural Networks (CNNs) has shown a really strong potential to provide automated features extraction and classification in the context of remote sensing. One recent and apparently efficient approach to reducing the data scarcity in specialised fields is transfer learning, which capitalises on knowledge acquired by large-scale pre-trained models like ResNet-50, EfficientNet, and Xception to improve the generalisation with respect to limited training samples (Bai and Cui, 2023). ResNet architecture has been successfully utilised in remote sensing operations particularly in feature extraction by using the ResNet-50 architecture that is characterised by residual blocks and skip connexions that reduce vanishinggradients. However, hyper-parameter configuration such as learning rate, batch size, dropout rates, and weight decay is critically important to the performance of deep learning models, and in both grid and random search strategies, conventional methods are computationally inefficient and find local optima, especially in high-dimensional search spaces of a typical deep neural network (Wang and Ren, 2022).

1.4. Bayesian Optimization for Automated Tuning

The Bayesian Optimization (BO) has emerged as a sample-efficient algorithm for black-box optimisation tasks, providing a principled probabilistic model of hyperparameter tuning. Through building a surrogate model, which is often a Gaussian Process that attempts to model the unknown objective function, BO trades off between exploring unexplored parameter space and exploiting promising parameter combinations by using an acquisition function like Expected Improvement (EI) or Upper Confidence Bound (UCB). More recent implementation of BO in deep learning settings, such as the BO-DRNet system to detect oil spills, have shown better convergence behaviour and improved semantic segmentation quantitatively compared to traditional tuning methods (Wang and Ren, 2022). Combining BO with transfer learning pipelines presents an interesting chance to overcome computational bottlenecks and sub-optimal configurations that limit the use of SAR-based oil spill detection systems presently.

1.5. Proposed Contribution and Paper Organization

The present manuscript suggests an optimised transfer-learning architecture, which harnesses the power of feature-extraction of ResNet-50 with the automated, hyperparameter-tuning capabilities of Bayesian Optimisation. The methodology overcomes three severe limitations of the existing methodologies: (1) the computational cost of manual hyperparameter optimization, (2) the challenge of identifying oil spills in clustered look-alike behaviour, and (3) the problem of highly unbalanced maritime remote-sensing data. The current study measures the proposed pipeline on the recently available dataset of Sentinel1 Eastern Mediterranean Sea, with 3225 labelled oil objects on 1,365 patches and 2,990 look-alike patches, which is structured using K-means clustering (Yang and Schütte, 2025).

2. LITERATURE REVIEW

This section reviews existing literature across three critical domains: deep learning architectures for marine oil spill detection, transfer learning strategies for remote sensing feature extraction, and Bayesian Optimization techniques for neural network hyperparameter tuning. The synthesis of these research streams motivates our integrated approach.

2.1. Deep Learning in Marine Oil Spill Detection

Deep learning has been applied to marine oil spill detection, with significant strides in the recent years due to the growing access to high-resolution SAR images and the development of neural-network models (Yang and Schütte, 2025). Initial models were dominated by traditional machine-learning methods like support-vector machines and random forests that required a laborious level of hand-designed feature engineering and were unable to as effectively model the inherent variability of oceanic surface processes. Deep-learning frameworks have enabled end-to-end feature learning to achieve a significantly higher level of detection accuracy in non-trivial maritime scenarios (Wang and Ren, 2022). Modern paradigms have explored various architectural paradigms in the detection of oil-spills using SAR. Convolutional Neural Networks (CNNs) have been specifically shown to effectively represent spatial hierarchies of dark spots features, with more elaborate models featuring a greater capability to differentiate fine textual variation between oil slicks and look-alike occurrences (Yang and Schütte, 2025). The bottleneck in functioning detection systems is the challenge of look-alike discrimination: it is necessary to distinguish between biogenic films, low-wind zones, internal waves, and rain cells and the hydrocarbon spills (Wang and Ren, 2022).

U-Net and DeepLabV3 semantic-segmentation architectures have been modified to pixel-level oil-spill delineation allowing the ability to detect a boundary accurately (which is required to measure the extent of spillage) (Yang and Schütte, 2025). Object-detection models such as Faster R- CNN and YOLO versions have also been implemented at the instance level, and have been found especially useful in detecting multiple discrete spill events across large swaths of SAR. The paper by Wang and Ren (2022) about BO-DRNet is an important step in this direction, as it has been shown that specialised deep residual networks that are optimised to SAR polarimetric features can have higher than generic computer-vision networks. Nonetheless, the current deep-learning solutions to oil-spill identification

have several drawbacks: they tend to work with suboptimal hyperparameter settings and do not take into account the inherent statistical characteristics of the SAR images (Bai and Cui, 2023). Multiplicative noise of speckle noise of coherent radar systems, dynamic-range compression of GRD products, and anisotropic texture patterns of oceanic processes require domain-specific architectural adaptations, which have not been fully explored in the existing literature (Yang and Schütte, 2025).

2.2. Transfer Learning for Feature Extraction in Remote Sensing

Transfer learning has become a core paradigm of alleviating data scarcity in specialised remote-sensing tasks, using the representations that are learned on large natural-image data sets to improve performance on domain-specific tasks with small training sets (Bai and Cui, 2023). Its original idea is to pre-train deep neural networks with large-scale data processing data sets, as in ImageNet, and subsequently fine-tune the learned features to your desired applications, which is especially useful in remote sensing, the annotated data of which is both expensive and time-intensive to generate (Yang and Schütte, 2025).

Given a source domain $D_S = \{X_S, P(X_S)\}$ with source task $T_S = \{Y_S, f_S(\cdot)\}$ and target domain $D_T = \{X_T, P(X_T)\}$ with target task $T_T = \{Y_T, f_T(\cdot)\}$, transfer learning aims to improve the learning of the target predictive function $f_T(\cdot)$ using knowledge acquired from D_S and T_S, where $D_S \neq D_T$ or $T_S \neq T_T$ (Bai and Cui, 2023). In the context of CNNs, this typically involves transferring parameters θ_S learned on the source domain to initialize parameters θ_T for the target domain:

$\theta_T^{(0)} = \theta_S$ (1)

The fine-tuning process then optimizes these parameters with respect to the target task loss function L_T:

$\theta_T^* = arg\min_{\theta_T} L_T(f(X_T; \theta_T), Y_T)$ (2)

where X_T represents the target domain SAR imagery and Y_T denotes the corresponding oil spill labels (Wang and Ren, 2022).

Pre-trained models including ResNet-50, EfficientNet, and Xception have been extensively utilized across various remote sensing domains (Bai and Cui, 2023). The residual learning framework of ResNet-50, with its 50-layer architecture incorporating skip connections and batch normalization, has proven especially effective for capturing hierarchical visual features that transfer robustly across imaging modalities (Wang and Ren, 2022). For a residual block l, the mapping is defined as:

$y_l = F(x_l, \{W_l\}) + x_l$ (3)

$x_{l+1} = \sigma(y_l)$ (4)

where F represents the residual mapping to be learned, W_l denotes the layer weights, and σ indicates the activation function (Bai and Cui, 2023). These skip connections mitigate the vanishing gradient problem, enabling effective training of deep networks essential for complex feature extraction.

Feature-based transfer learning, wherein the pre-trained network serves as a fixed feature extractor followed by task-specific classification layers, offers computational efficiency and reduced risk of overfitting on small datasets (Yang and Schütte, 2025). However, the optimal depth of feature extraction and the degree of fine-tuning required remain empirical questions

dependent on dataset size and task complexity. For a feature extractor $\phi(\cdot;\theta_{frozen})$ with frozen parameters and a task-specific head $g(\cdot;\theta_{trainable})$, the prediction is formulated as:

$\widehat{y} = g(\phi(x;\theta_{frozen});\theta_{trainable})$ (5)

According to the latest research findings, partial fine-tuning, which involves the freezing of early convolutional blocks and freezing of later layers, also offers an optimal tradeoff between generic representations and domain-specific features (Bai and Cui, 2023). The given strategy is particularly relevant to SAR oil-spill detection, in which the visual appearance of dark spots can be significantly different as compared to natural-image categories but still has the basic geometric and textural characteristics (Yang and Schütte, 2025).

2.3. Bayesian Optimization in Neural Networks

Bayesian Optimization (BO), has proven itself to be a more effective choice of hyperparameter optimization in machine-learning systems, especially when the objective-function can only be evaluated in a computationally-intensive manner (Bai and Cui, 2023). In contrast to grid search, which evaluates all combinations of parameters, or random search, which draws samples of configurations with no use of previous evaluations, BO uses probabilistic surrogate models of the objective landscape to guide an intelligent exploration (Wang and Ren, 2022).

The BO procedure aims to find the global optimum of an unknown objective function $f: X \to R$ over a hyperparameter space $X \subseteq R^d$:

$x^* = arg\max_{x\in X} f(x)$ (6)

where f represents the validation metric (IoU or F1-score) and x denotes the vector of hyperparameters including learning rate η, batch size B, dropout rate p, and weight decay λ (Bai and Cui, 2023). Due to the expensive nature of evaluating f, BO employs a surrogate model to approximate the objective surface.

The theoretical foundations of BO rely on Gaussian Process (GP) priors to model the unknown objective function, capturing uncertainty in predictions to balance exploration of high-uncertainty regions against exploitation of promising configurations (Wang and Ren, 2022). A GP is defined as a collection of random variables, any finite number of which have a joint Gaussian distribution:

$f(x) \sim GP(m(x), k(x,x'))$ (7)

where $m(x) = E[f(x)]$ is the mean function and $k(x,x') = E[(f(x)-m(x))(f(x')-m(x'))]$ is the covariance function or kernel (Bai and Cui, 2023). Given observed data $D_n = \{(x_i, y_i)\}_{i=1}^n$ where $y_i = f(x_i) + \epsilon_i$ with Gaussian noise $\epsilon_i \sim N(0, \sigma_n^2)$, the posterior distribution at a new point x_* is:

$f(x_*)|D_n, x_* \sim N(\mu_n(x_*), \sigma_n^2(x_*))$ (8)

with posterior mean and variance:

$\mu_n(x_*) = k_*^T (K + \sigma_n^2 I)^{-1} y$ (9)

$\sigma_n^2(x_*) = k(x_*, x_*) - k_*^T (K + \sigma_n^2 I)^{-1} k_*$ (10)

where K is the $n \times n$ covariance matrix with entries $K_{ij} = k(x_i, x_j)$ and $k_* = [k(x_*, x_1), \ldots, k(x_*, x_n)]^T$ (Bai and Cui, 2023).

Acquisition functions formalize the exploration-exploitation trade-off, enabling automated selection of the next hyperparameter configuration to evaluate (Wang and Ren, 2022). The Expected Improvement (EI) acquisition function is defined as:

$\alpha_{EI}(x; D_n) = E[\max(f(x) - f(x^+), 0)]$ (11)

where $f(x^+) = \max_{i \leq n} f(x_i)$ is the current best observed value. Under the GP posterior, this has a closed form:

$\alpha_{EI}(x) = (\mu_n(x) - f(x^+))\,\Phi(Z) + \sigma_n(x)\phi(Z)$ (12)

where $Z = (\mu_n(x) - f(x^+))/\sigma_n(x)$, and Φ and ϕ are the standard normal cumulative distribution and probability density functions, respectively (Bai and Cui, 2023).

Alternatively, the Upper Confidence Bound (UCB) acquisition function incorporates an exploration parameter β:

$\alpha_{UCB}(x; D_n) = \mu_n(x) + \sqrt{\beta}\sigma_n(x)$ (13)

In Wang and Ren (2022), it is shown that BO is applied to deep residual networks to detect oil-spills, with automated hyperparameter tuning being able to significantly increase Intersection-over-Union (IoU) and decrease False Discovery rate compared to manually tuned baselines. Their BO-DRNet architecture uses Bayesian Optimization to pretrain deep residual networks to extract polarimetric SAR features especially in semantic-segmentation tasks, where the networks provide better performance in semantic-segmentation and classification (Wang and Ren, 2022).

There are distinctive issues that arise due to the high-dimensionality of the hyperparameter space of neural-networks and stochasticity of training processes when integrating BO with deep-learning pipelines (Bai and Cui, 2023). To minimise computing cost, multi-fidelity optimization methods that utilise the partial training executions as approximations of the final performance have been developed. Bai *et.al.* (2023) review the current developments in transfer learning, which is used in Bayesian Optimization, where meta-learning methods have the capacity to further speed up an optimization process by utilising knowledge acquired in related tasks or data.

2.4. Research Gaps and Motivation

Although the literature summarised has taken important steps toward using deep learning to detect oil -spill, transfer learning to remote sensing, and Bayesian Optimization of neural networks, some key gaps that need to be addressed have not been done so (Yang and Schütte, 2025). To begin with, these three streams of research, which include transfer learning based on ResNet-50, Bayesian Optimization, and SAR-specific oil-spill detection are not fully investigated (Wang and Ren, 2022). Majority of the existing methods either use transfer learning without explicit hyperparameter optimization or use BO over architectures in general without using pre-trained representations (Bai and Cui, 2023). Again, there is less analysis of the detection algorithms on datasets with realistic look-alike diversity (Yang and Schütte, 2025). Yang and Schütte (2025) overcome this shortcoming by their K-means clustered set of Eastern Mediterranean SAR images that is a strict standard to evaluate the false-positive suppression of various oceanic phenomena. Nonetheless, it is still not determined how optimised transfer-learning pipelines will perform on this challenging dataset (Wang and Ren, 2022). The financial efficiency of hyperparameter search algorithms with regard to oil-spil detection should be systematically compared (Bai and Cui, 2023). Although BO has been shown to have benefits in other areas, convergence properties of BO compared to grid and random search on ResNet-50 with imbalanced SAR datasets need empirical verification (Wang and Ren, 2022).

This work addresses these gaps by proposing a unified framework that combines ResNet-50 transfer learning with Bayesian Optimization, evaluated on a comprehensive dataset with clustered look-alikes (Yang and Schütte, 2025). This integration aims to deliver both improved detection accuracy and computational efficiency, advancing the state-of-the-art in automated oil spill monitoring systems (Bai and Cui, 2023; Wang and Ren, 2022).

3. DATASET AND PREPROCESSING

Both the efficiency and the robustness of any deep-learning model, especially in the context of oil spill identification with the help of satellites, are limited by the quality and variety of the underlying data (Shaban and El-Baz, 2021). The current research uses a detailed dataset which is curated on Sentinel -1 Synthetic Aperture Radar (SAR) imaging, which is created to detect the high level of variability in the marine settings.

3.1. Dataset Description

3.1.1. It contains 3,166 oil spill samples that are well-annotated (Huang and Perrie, 2025). To obtain strong model generalisation, as well as explicitly to solve the problem of look-alikes, including low-wind regions, biogenic films and atmospheric phenomena that often result in false detections, the dataset contains high percentage of negative samples (non-oil dark spots). Such samples are crucial to the way the model is trained to differentiate between actual oil slicks and the natural surface features (Genovez and Miranda, 2023). The data covers different environmental factors, such as the varying wind velocity and different levels of the sun glint that is essential in assessing the performance of the model under realistic environment (Du and Yang, 2025; Huang and Perrie, 2025).

3.2. Data Preprocessing

To prepare the SAR data for the ResNet-50 backbone, several preprocessing steps are implemented to standardize the input and enhance the model's ability to extract high-level features.

i. **Geometric and Radiometric Correction:** The raw SAR images undergo radiometric calibration and thermal noise removal to ensure consistent backscatter values across the entire dataset. Border noise, which can introduce artifacts, is removed during the initial processing stage (Huang and Perrie, 2025).

ii. **Normalization and Scaling:** Given the wide range of backscatter intensities in SAR imagery, the data is normalized to a standard range [0, 1]. This is crucial for maintaining numerical stability during the training of deep learning architectures and improving convergence speed (Luo and Chen, 2025).

iii. **Data Augmentation:** To mitigate the issues of data scarcity and class imbalance, the dataset is expanded using a variety of augmentation techniques. Spatial transformations, including horizontal/vertical flips and random rotations, are applied to the

training set. These transformations increase the variance of the input data, helping the model learn features that are invariant to the orientation of the oil slick, thereby improving the overall robustness and generalization capability of the final model (Subramanian and Nandhini, 2022; Duan and Li, 2022).

3.3. Proposed Model Architecture

The suggested model design combines feature-based transfer learning with a hyperparameter optimization engine in order to classify marine oil spills in SAR images. In its most basic form, the model makes use of a pre-trained version of ResNet-50 as a frozen convolutional feature extractor. This allows the model to make use of powerful, hierarchical visual representations trained on large-scale data, and reduce the calculations needed as well as the risk of overfitting the model to the specialised SAR data. The obtained features are then forwarded to a customised, lightweight, classification head consisting of 256-unit fully connected (Dense) layer, a regularisation Dropout layer, and a final Sigmoid activation layer to produce a binary prediction (Oil Spill versus Non-Oil). A Bayesian Optimisation engine is also dynamically connected with the training loop to maximise predictive performance and generalisation. This engine progressively optimises validation metrics to optimally tune crucial hyperparameters, namely, the type of optimiser, learning rate, weight decay, dropout rate, and momentum, thus such that the model fits best to the intricate textual characteristics of oceanic look-alikes and realistic oil slicks. The model architecture is shown in Figure 1.

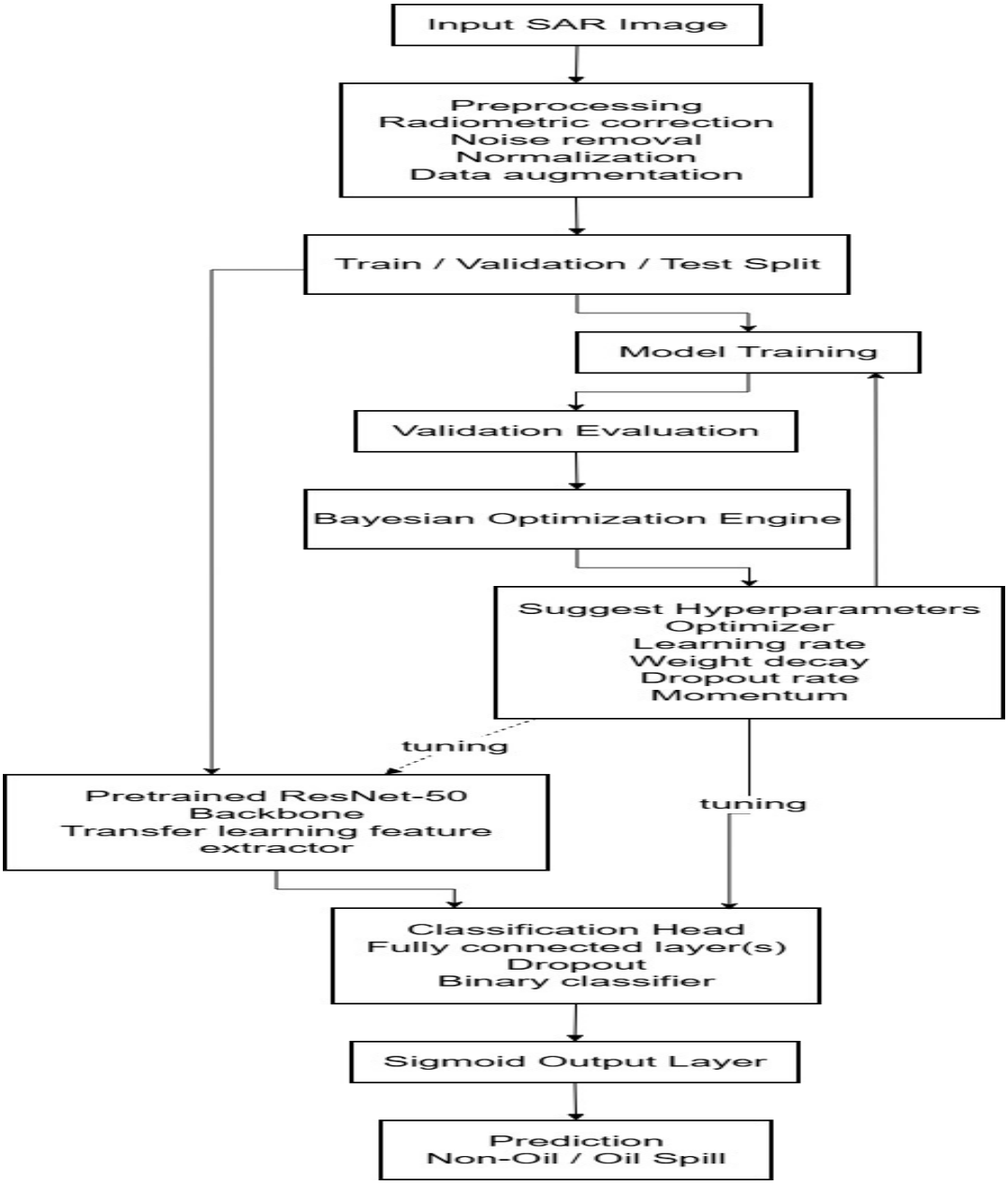

Figure 1: Proposed Model Architecture

4. RESULT

4.1. Dataset Class Distribution

The evaluation dataset exhibits a distinct class imbalance that represents real-world marine environments. The Non-Oil class constitutes the majority with approximately 2,300 images, while the Oil Spill class contains roughly 1,300 images.

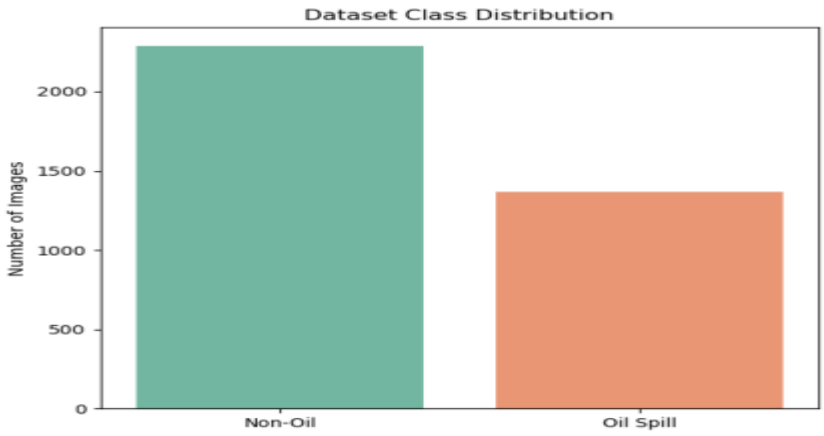

Figure 2: Dataset Class Distribution for Non-Oil and Oil Spill Samples.

4.2. Hyperparameter Optimization

Bayesian optimization significantly altered the baseline training configuration to enhance the model's generalization capabilities. The optimizer was switched from Adam to Stochastic Gradient Descent (SGD), and specific values for weight decay, dropout, and momentum were introduced to explicitly regularize the network.

Table 1. Hyperparameters before and after optimization

Hyperparameter	Before Optimization	After Optimization
Optimizer	Adam	SGD
Learning Rate	0.001	0.001578
Weight Decay	0.0	0.012348
Dropout Rate	0.0	0.0129
Momentum	Not Used	0.5872

4.3. Model Training and Convergence

The learning curves demonstrate stable convergence across the five training epochs for the optimized ResNet-50 architecture. Training and validation loss decreased steadily without diverging, while validation accuracy climbed concurrently to match the training accuracy at approximately 85%. This tight alignment between training and validation metrics suggests the applied regularization successfully prevented overfitting.

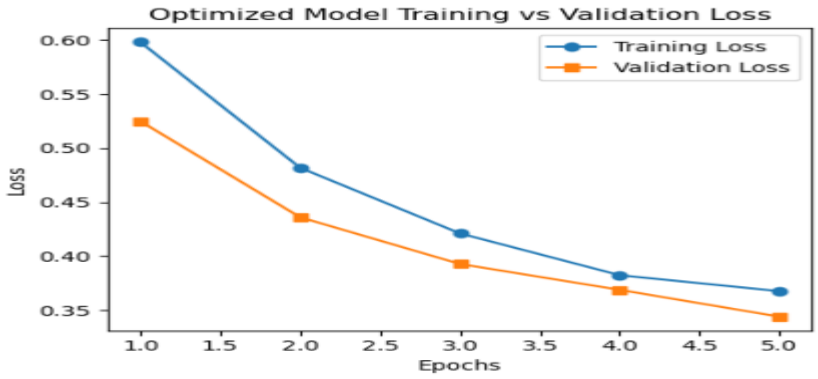

Figure 3: Optimized Model Training vs. Validation Loss.

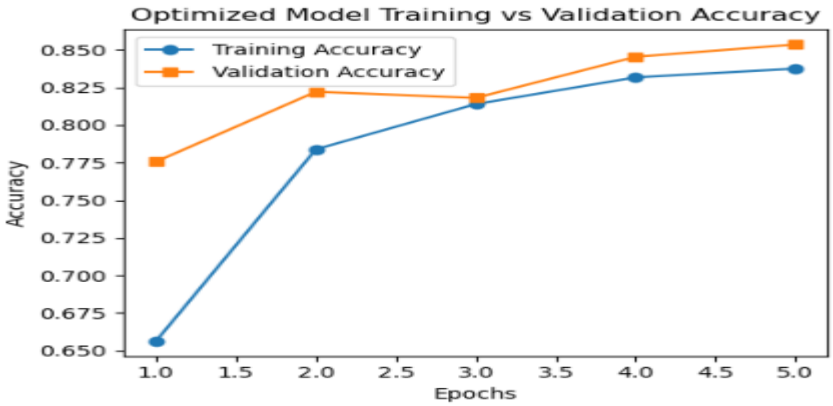

Figure 4: Optimized Model Training vs. Validation Accuracy.

4.4. Confusion Matrix Analysis

The confusion matrix details the exact distribution of accurate and misclassified predictions across both classes. Out of the total evaluation samples, the model correctly identified 421 Non-Oil regions and 203 actual Oil Spills. The model recorded 57 false negatives (oil classified as non-oil) and 50 false positives (non-oil classified as oil), showing a slightly conservative bias regarding spill detection.

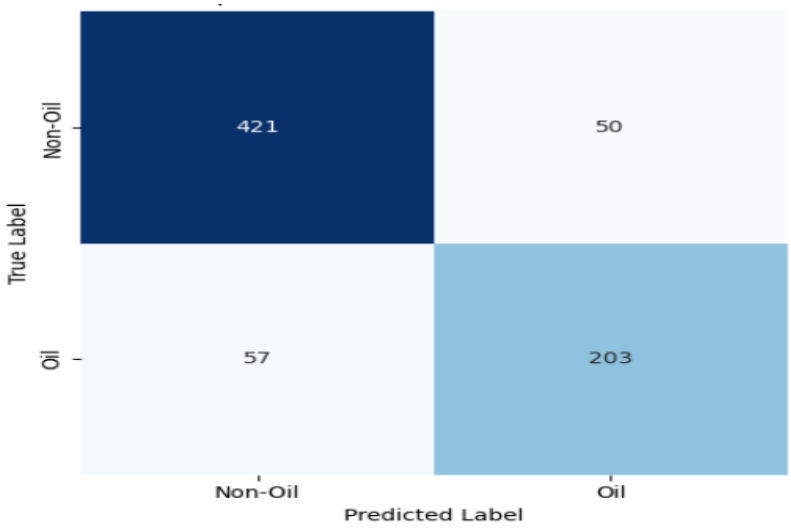

Figure 5: Optimized Model Confusion Matrix.

4.5. Classification Report

A breakdown of the classification report reveals that the model performs more reliably on the majority class. The Non-Oil class achieved an F1-score of 0.89, whereas the Oil class achieved an F1-score of 0.79.

Table 2. The Classification Report

Class	Precision	Recall	F1-Score	Support
Non-Oil (0)	0.88	0.89	0.89	471
Oil (1)	0.80	0.78	0.79	260
Accuracy			0.85	731
Macro Average	0.84	0.84	0.84	731
Weighted Average	0.85	0.85	0.85	731

The ResNet-50 model that was optimised using Bayesian methods showed high and consistent performance in the identification of oil spills with an overall accuracy and weighted F1-score of about 85.3 per cent. The convergence and strong generalisation of the training process were steady and without overfitting. Nevertheless, the model had a slightly high performance of identifying non-oil regions (F1-score = 0.89) than real oil spills (F1-score = 0.79) which shows a greater discriminatory power of most non-oil category.

5. CONCLUSION

This paper introduces an optimised transfer-learning structure that effectively combines a pre-trained ResNet-50 model with Bayesian hyper-parameter optimisation to solve a complicated problem of marine oil spills in SAR data. The suggested model can discriminate uniquely between real oil slicks and widespread oceanic look-alikes and achieves a strong

overall accuracy of 85.36 per cent and a weighted F1-score of 85.32 per cent by automating the selection of critical training parameters. The Bayesian optimisation engine was added to guarantee consistency of model convergence and reduce the effects of over-fitting and it was very successful at searching the complex hyper-parameter space of SAR-based deep learning. Though the results of the classification show a slight bias toward conservativeness (F1-score=.89) with the model performing better on the majority group (non-oil spill class) (F1-score=.89) than on the minority group (oil spill class) (F1-score=.79), these statistics do not indicate the model was deficient in reliability between false positives and false negatives. Finally, this computationally and automated pipeline is a state of the art in operational maritime surveillance, providing a scalable operational solution to real time environmental surveillance and quick disaster recovery. Future studies can address more sophisticated data-balancing methods or be able to multi-sense to increase the sensitivity of detection in the minority oil spill category.

References

Li Y. Shen Y. Zhang X. Zhang W. Bai, T. and B. Cui. Transfer learning for bayesian optimization: A survey. *arXiv*. https://doi.org/10.48550/arxiv.2302.05927. 2023.

Ma Y. Li Z. Liu R. Jiang Z. Du, K. and J. Yang. Ms3osd: A novel deep learning approach for oil spills detection using optical satellite multisensor spatial-spectral fusion images. *IEEE Journal of Selected Topics in Applied Earth Observations and Remote Sensing*. https://doi.org/10.1109/jstars.2025.3550421. 2025.

Xie Z. Kang X. Duan, P. and S. Li. Self-supervised learning-based oil spill detection of hyperspectral images. *Science China Technological Sciences*. https://doi.org/10.1007/s11431-021-1989-9. 2022.

de Araújo Ponte F. F. de Oliveira Matias Í. Torres-S. B. Beisl C. Mano M. Silva G. M. A. Genovez, P. and F. Miranda. Development and application of predictive models to distinguish seepage slicks from oil spills on sea surfaces employing sar sensors and artificial intelligence: Geometric patterns recognition under a transfer learning approach. *Remote Sensing*. https://doi.org/10.3390/rs15061496. 2023.

Zhang B. Huang, X. and W. Perrie. A two-stage deep learning method for marine oil spill localization and segmentation from synthetic aperture radar images. *IEEE Journal of Selected Topics in Applied Earth Observations and Remote Sensing*. https://doi.org/10.1109/jstars.2025.3567859. 2025.

Abdul Majeed A. P. P. Omar Z. Aslam S. Luo, Y. and Y. Chen. Computationally efficient transfer learning pipeline for oil palm fresh fruit bunch defect detection. *Technologies*. https://doi.org/10.3390/technologies13060234. 2025.

Salim R. Khalifeh H. A. Khelifi A. Shalaby A. El-Mashad S. Y. Mahmoud A. M. Ghazal M. Shaban, M. and A. El-Baz. A deep-learning framework for the detection of oil spills from sar data. *Sensors*. https://doi.org/10.3390/s21072351. 2021.

Shanmugavadivel K. Subramanian, M. and P. S. Nandhini. On fine-tuning deep learning models using transfer learning and hyper-parameters optimization for disease identification in maize leaves. *Neural Computing and Applications*. https://doi.org/10.1007/s00521-022-07246-w. 2022.

Wan J. Liu S. Chen Y. Yasir M. Xu M. Wang, D. and P. Ren. Bo-drnet: An improved deep learning model for oil spill detection by polarimetric features from sar images. *Remote Sensing*. https://doi.org/10.3390/rs14020264. 2022.

Singha S. Goldman R. Yang, Y.-J. and F. Schütte. Dataset of oil slicks, look-alikes and remarkable sar signatures obtained from sentinel-1 data in the eastern mediterranean sea. *Earth System Science Data*. 2025.